Supplementary Material for

Kinetics, DFT Study and Antibacterial Activity of Zinc(II) and Copper(II) Terpyridine Complexes

Enisa Selimović,[1] Svetlana Jeremić,[1] Braho Ličina,[2] and Tanja Soldatović[1,*]

[1] Department of Chemical-Technological Science, State University of Novi Pazar, Vuka Karadžića bb, 36300 Novi Pazar, Serbia

[2] Department of Biomedical Science, State University of Novi Pazar, Novi Pazar, Vuka Karadžića bb, 36300 Novi Pazar, Serbia

[*] Email: tsoldatovic@np.ac.rs; Tel.: +381-20-317-754; Fax: +381-20-337-0669

Table S1. Observed pseudo-first order rate constants as a function of nucleophile concentration for the substitution reactions of [$ZnCl_2$(terpy)] complex with 5'-IMP at pH 7.38 (0.005 mol L^{-1} phosphate buffer) in the addition of 0.010 mol L^{-1} NaCl at 22°C.

Complex	λ/nm	10^3 $C_{5'\text{-IMP}}$ [mol L^{-1}]	10^4 k_{obsd1} [s^{-1}]	10^4 k_{obsd2} [s^{-1}]
[$ZnCl_2$(terpy)]	320	1	180.0(4)[a]	32.0(4)[a]
		2	250.0(4)	54.0(4)
		3	350.0(4)	76.0(4)
		4	520.0(4)	90.0(4)
		5	690.0(4)	130.0(4)

[a]Number of runs in parenthesis.

Table S2. Observed pseudo-first order rate constants as a function of nucleophile concentration for the substitution reactions of [$ZnCl_2$(terpy)] complex with 5'-GMP pH 7.38 (0.005 mol L^{-1} phosphate buffer) in the addition of 0.010 mol L^{-1} NaCl at 22°C.

Complex	λ/nm	10^3 $C_{5'\text{-GMP}}$ [mol L^{-1}]	10^4 k_{obsd1} [s^{-1}]	10^4 k_{obsd2} [s^{-1}]
[$ZnCl_2$(terpy)]	312	1	220.0(4)[a]	39.0(4)[a]
		2	330.0(4)	59.0(4)
		3	450.0(4)	71.0(4)
		4	626.0(4)	90.0(4)
		5	800.0(4)	110.0(4)

[a]Number of runs in parenthesis.

Table S3. Observed pseudo-first order rate constants as a function of nucleophile concentration for the substitution reactions of [$ZnCl_2$(terpy)] complex with L-Met at pH 7.38 (0.005 mol L^{-1} phosphate buffer) in the addition of 0.010 mol L^{-1} NaCl at 22°C.

Complex	λ/nm	10^3 $C_{L\text{-}Met}$ [mol L^{-1}]	10^4 k_{obsd1} [s^{-1}]	10^4 k_{obsd2} [s^{-1}]
[$ZnCl_2$(terpy)]	264	1	33.0(4)[a]	6.64(4)[a]
		2	38.2(4)	9.70(4)
		3	59.7(4)	12.8(4)
		4	87.1(4)	19.0(4)
		5	120.7(4)	38.6(4)
			102.1(4)[b]	35.2(4)[b]
			80.1(4)[c]	29.1(4)[c]

[a]Number of runs in parenthesis.
[b]Observed pseudo-first order rate constants at 289 K.
[c]Observed pseudo-first order rate constants at 281 K.

Table S4. Observed pseudo-first order rate constants as a function of nucleophile concentration for the substitution reactions of [$ZnCl_2$(terpy)] complex with DL-Asp pH 7.38 (0.005 mol L^{-1} phosphate buffer) in the addition of 0.010 mol L^{-1} NaCl at 22°C.

Complex	λ/nm	10^3 $C_{DL\text{-}Asp}$ [mol L^{-1}]	10^4 k_{obsd1} [s^{-1}]	10^4 k_{obsd2} [s^{-1}]
[$ZnCl_2$(terpy)]	281	1	955.5(4)[a]	80.2(4)[a]
		2	1623.0(4)	159.4(4)
		3	2407.0(4)	245.4(4)
		4	3244.8(3)	327.0(3)
		5	4110.0(4)	360.6(4)

[a]Number of runs in parenthesis.

Table S5. Observed *pseudo*-first order rate constants as a function of nucleophile concentration for the substitution reactions of [$ZnCl_2$(terpy)] complex with GSH at pH 7.38 (0.005 mol L^{-1} phosphate buffer) in the addition of 0.010 mol L^{-1} NaCl at 22°C.

Complex	λ/nm	10^3 $C_{Znterpy}$ [mol L^{-1}]	10^4 k_{obsd1} [s^{-1}]	10^4 k_{obsd2} [s^{-1}]
[$ZnCl_2$(terpy)]	281	1	1711.9(4)[a]	119.6(4)[a]
		2	3378.5(4)	97.4(4)
		3	4088.6(4)	118.3(4)
		4	4545.5(5)	99.8(5)
		5	4670.0(5)	112.9(5)

[a]Number of runs in parenthesis.

Table S6. Observed pseudo-first order rate constants as a function of nucleophile concentration for the substitution reactions of [$CuCl_2$(terpy)] complex with 5'-IMP pH 7.38 (0.005 mol L^{-1} phosphate buffer) in the addition of 0.010 mol L^{-1} NaCl at 22°C.

[a]Number of runs in parenthesis.

Complex	λ/nm	10^3 $C_{5'\text{-IMP}}$ [mol L^{-1}]	10^4 k_{obsd1} [s^{-1}]	10^4 k_{obsd2} [s^{-1}]
[$CuCl_2$(terpy)]	352	1	362.0(4)[a]	80.7(4)[a]
		2	603.2(4)	268.8(4)
		3	876.8(4)	383.0(4)
		4	1174.1(5)	436.7(5)
		5	1500.0(4)	576.0(4)

Table S7. Observed pseudo-first order rate constants as a function of nucleophile concentration for the substitution reactions of [$CuCl_2$(terpy)] complex with 5'-GMP pH 7.38 (0.005 mol L^{-1} phosphate buffer) in the addition of 0.010 mol L^{-1} NaCl at 22°C.

[a]Number of runs in parenthesis

Complex	λ/nm	10^3 $C_{5'\text{-GMP}}$ [mol L^{-1}]	10^4 k_{obsd1} [s^{-1}]	10^4 k_{obsd2} [s^{-1}]
[$CuCl_2$(terpy)]	330	1	426.6(4)[a]	56.3(4)[a]
		2	699.2(4)	75.6(4)
		3	904.4(4)	99.9(4)
		4	1271.2(4)	130.0(4)
		5	1537.8(4)	151.9(4)

Table S8. Observed pseudo-first order rate constants as a function of nucleophile concentration for the substitution reactions of [$CuCl_2$(terpy)] complex with L-Met pH 7.38 (0.005 mol L^{-1} phosphate buffer) in the addition of 0.010 mol L^{-1} NaCl at 22°C.

Complex	λ/nm	10^3 $C_{L\text{-}Met}$ [mol L^{-1}]	10^4 k_{obsd1} [s^{-1}]	10^4 k_{obsd2} [s^{-1}]
[$CuCl_2$(terpy)]	250	1	191.6(4)[a]	29.6(4)[a]
		2	306.0(4)	60.1(4)
		3	504.0(4)	90.8(4)
		4	835.0(4)	121.6(4)
		5	958.0(4)	179.5(4)
			742.8(4)[b]	97.7(4)[b]
			269.3(4)[c]	15.40(4)[c]

[a] Number of runs in parenthesis.
[b]Observed pseudo-first order rate constants at 289K.
[c]Observed pseudo-first order rate constants at 281 K.

Table S9. Observed pseudo-first order rate constants as a function of nucleophile concentration for the substitution reactions of [$CuCl_2$(terpy)] complex with DL-Asp at pH 7.38 (0.005 mol L^{-1} phosphate buffer) in the addition of 0.010 mol L^{-1} NaCl at 22°C.

Complex	λ/nm	10^3 $C_{DL\text{-}Asp}$ [mol L^{-1}]	10^4 k_{obsd1} [s^{-1})	10^4 k_{obsd2} [s^{-1}]
[$CuCl_2$(terpy)]	333	1	1429.7(4)[a]	951.4(4)[a]
		2	2502.1(4)	1195.1(4)
		3	3268.9(4)	1785.5(4)
		4	4291.1(4)	2231.4(4)
		5	5319.5(4)	2812.2(4)

[a] Number of runs in parenthesis.

Table S10. Observed pseudo-first order rate constants as a function of nucleophile concentration for the substitution reactions of [$CuCl_2$(terpy)] complex with GSH at pH 7.38 (0.005 mol L^{-1} phosphate buffer) in the addition of 0.010 mol L^{-1} NaCl at 22°C.

Complex	λ/nm	10^3 $C_{Cuterpy}$ [mol L^{-1}]	10^4 k_{obsd1} [s^{-1}]	10^4 k_{obsd2} [s^{-1}]
[$CuCl_2$(terpy)]	280	1	1425.1(4)[a]	581.0(4)[a]
		2	2774.0(4)	897.6(4)
		3	4681.0(4)	1041.1(4)
		4	6626.9(4)	1608.5(4)
		5	8551.0(4)	2035.8(4)

[a] Number of runs in parenthesis.

Table S11. Experimental and calculated electronic transitions for $[ZnCl_2(terpy)]$ and $[ZnCl_2(terpy)]\cdot H_2O$ calculated in aqueous solution; λ – wavelength in nm, f – oscillator strength.

Experimental	M06/6-311++G(d,p)					
	$[ZnCl_2(terpy)]$			$[ZnCl_2(terpy)]\cdot H_2O$		
λ	λ	*f*	Leading configurations	λ	*f*	Leading configurations
337	315.3	0.4150	H→L (69%)	315.7	0.4082	H→L (69%)
319	281.7	0.2232	H→L+1 (68%)	281.7	0.2254	H→L+1 (68%)
280	249.8	0.1697	H-6→L+1 (64%)	248.5	0.1018	H-6→L+1 (56%)
236	240.2	0.1785	H→L+3 (48%)	239.9	0.1749	H→L+3 (50%)
			H-6→L+1 (21%)			H-6→L+1 (21%)

Table S12. Experimental and calculated electronic transitions for $[CuCl_2(terpy)]$ and $[CuCl_2(terpy)]\cdot H_2O$ calculated in aqueous solution; λ – wavelength in nm, f – oscillator strength.

Experimental	M06/6-311++G(d,p)					
	$[CuCl_2(terpy)]$			$[CuCl_2(terpy)]\cdot H_2O$		
λ	λ	*f*	Leading configurations	λ	*f*	Leading configurations
357	347	0.0265	H→L (80%)	342.9	0.0296	H→L (80%)
415	469.4	0.0011	H-1→L (86%)	365.3	0.0020	H-1→L (22%)
684	869.7	0.0016	H-4→L (59%)	860.5	0.0017	H-4→L (55%)

Table S13. Donor (Lewis type) and acceptor (non-Lewis type) NBOs in [$ZnCl_2$(terpy)] labelad as Zn(II), [$ZnCl_2$(terpy)](aq) labeled as $Zn(II)_{aq}$ and [$ZnCl_2$(terpy)]·H_2O(aq) labeled as Zn(II)·H_2O complexes. E(2) stands for the second order interaction energy between the donor and acceptor NBOs.

Donor Lewis type	**Occupancy Donor Lewis type NBO**			**Aceptor non Lewis type**	**Occupancy Aceptor non Lewis type NBO**			**$E^{(2)}$ [kJ mol^{-1}]**		
Molecular orbital	Zn(II)	$Zn(II)_{aq}$	Zn(II)·H_2O	**Molecular orbital**	Zn(II)	$Zn(II)_{aq}$	Zn(II)·H_2O	Zn(II)	$Zn(II)_{aq}$	Zn(II)·H_2O
s Cl2	1.818	1.862	1.857	4s Zn	0.443	0.420	0.420	342.75	265.89	279.28
pz Cl1	1.813	1.847	1.856	4s Zn	0.443	0.420	0.420	365.72	301.33	278.86
sp^2 N3	1.889	1.884	1.883	4s Zn	0.443	0.420	0.420	105.35	123.76	125.77
sp^2 N2	1.888	1.878	1.878	4s Zn	0.443	0.420	0.420	98.11	132.13	130.92
sp^2 N1	1.889	1.884	1.884	4s Zn	0.443	0.420	0.420	105.35	123.76	126.19
π C14- C15	1.619	1.609	1.609	π* C11- N3	0.369	0.401	0.403	74.27	78.45	78.28
π C14- C15	1.619	1.609	1.609	π* C12- C13	0.294	0.283	0.283	98.78	95.86	95.86
π C14- C15	1.619	-	1.609	π* C7- N2	0.442	-	0.471	73.85	-	79.71
π C14- C15	-	1.609	-	π* C7- C8	-	0.318	-	-	53.14	-
π C11- N3	1.740	1.761	1.762	π* C14- C15	0.331	0.321	0.321	118.70	110.29	109.91
π C11- N3	1.740	1.761	1.762	π* C12- C13	0.294	0.283	0.283	50.29	46.32	45.90
π C12- C13	1.633	1.610	1.609	π* C14- C15	0.331	0.321	0.321	80.29	81.21	81.17
π C12- C13	1.633	1.610	1.609	π* C11- N3	0.369	0.401	0.403	134.52	148.57	149.49
π C6- C10	1.591	-	1.587	π* C7- N2	0.442	-	0.471	78.07	-	79.45
π C6- C10	1.591	-	1.587	π* C8- C9	0.299	-	0.278	104.01	-	97.74
π C6- C10	1.591	-	1.587	π* C3- C4	0.331	-	0.320	47.28	-	48.53
π C6- N2	-	1.752	-	π* C7- C8	-	0.318	-	-	111.50	-
π C6- N2	-	1.752	-	π* C9- C10	-	0.278	-	-	43.14	-
π C7- N2	1.730	-	1.752	π* C6- C10	0.327	-	0.317	118.45	-	111.17
π C7- N2	1.730	-	1.752	π* C8- C9	0.299	-	0.278	48.07	-	43.14
π C7- N2	1.730	-	1.752	π* C14- C15	0.331	-	0.321	38.41	-	36.36
π C9- C10	-	1.604	-	π* C6- N2	-	0.471	-	-	152.00	-
π C9- C10	-	1.604	-	π* C7- C8	-	0.318	-	-	78.07	-
π C8- C9	1.632	-	1.604	π* C6- C10	0.327	-	0.317	76.07	-	77.95
π C8- C9	1.632	-	1.604	π* C7- N2	0.442	-	0.471	137.03	-	151.67
π C7- C8	-	1.587	-	π* C6- N2	-	0.471	-	-	78.87	-
π C7- C8	-	1.587	-	π* C9- C10	-	0.278	-	-	97.78	-

π C7- C8	-	1.587	-	π* C14- C15	-	0.321	-	-	48.62	-
π C3- C4	1.619	-	1.609	π* C6- C10	0.327	-	0.317	52.84	-	53.01
π C3- C4	-	1.609	-	π* C6- N2	-	0.471	-	-	80.29	-
π C3- C4	1.619	1.609	1.609	π* C2- N1	0.369	0.401	0.402	74.27	78.45	78.32
π C3- C4	1.619	1.609	1.609	π* C1- C5	0.294	0.283	0.283	98.78	95.86	95.90
π C2- N1	1.740	1.761	1.762	π* C3- C4	0.331	0.321	0.320	118.70	110.29	109.91
π C2- N1	1.740	1.761	1.762	π* C1- C5	0.294	0.283	0.283	50.29	46.32	46.02
π C1- C5	1.633	1.610	1.610	π* C3- C4	0.331	0.321	0.320	80.29	81.21	81.04
π C1- C5	1.633	1.610	1.610	π* C2- N1	0.369	0.401	0.402	134.52	148.57	148.99
σ O- H	-	-	1.999	4s Zn	-	-	0.420	-	-	0.29
sp^3 O	-	-	1.993	4s Zn	-	-	0.420	-	-	1.92

Table S14. Donor (Lewis type) and acceptor (non-Lewis type) NBOs in [$CuCl_2$(terpy)] labelad as Cu(II), [$CuCl_2$(terpy)](aq) labeled as $Cu(II)_{aq}$ and [$CuCl_2$(terpy)]·H_2O(aq) labeled as Cu(II)·H_2O complexes. E(2) stands for the second order interaction energy between the donor and acceptor NBOs.

Donor Lewis type	**Occupancy Donor Lewis type NBO**			**Aceptor non Lewis type**	**Occupancy Aceptor non Lewis type NBO**			**$E^{(2)}$ [kJ mol^{-1}]**		
Molecular orbital	Cu(II)	$Cu(II)_{aq}$	Cu(II)·H_2O	**Molecular orbital**	Cu(II)	$Cu(II)_{aq}$	Cu(II)·H_2O	Cu(II)	$Cu(II)_{aq}$	Cu(II)·H_2O
s Cl2	1.996	-	-	4s Cu	0.360	-	-	34.10	-	-
py Cl2	1.980	-	-	4s Cu	0.360	-	-	52.72	-	-
pz Cl2	1.756	1.920	1.916	4s Cu	0.360	0.346	0.344	282.67	144.47	156.44
s Cl1	1.997	-	1.993	4s Cu	0.360	-	0.344	36.44	-	49.96
px Cl1	-	1.992	-	4s Cu	-	0.346	-	-	49.87	-
py Cl1	1.979	-	-	4s Cu	0.360	-	-	53.81	-	-
pz Cl1	1.748	1.780	1.796	4s Cu	0.360	0.346	0.344	334.47	306.81	284.97
sp^2 N3	1.818	-	-	dz^2 Cu	1.402	-	-	187.28	-	-
sp^2 N3	1.818	1.804	1.805	4s Cu	0.360	0.346	0.344	126.73	151.21	150.58
sp^2 N2	1.890	1.795	1.794	4s Cu	0.360	0.346	0.344	85.23	155.14	148.70
sp^2 N2	-	1.795	1.794	dz^2 Cu	-	1.383	1.379	-	572.20	568.27
sp^2 N1	1.818	-	-	dz^2 Cu	1.402	-	-	187.28	-	-
sp^2 N1	1.818	1.804	1.806	4s Cu	0.360	0.346	0.344	126.73	151.21	150.12
π C14- C15	1.620	1.616	1.615	π* C11- N3	0.378	0.404	40382.000	72.30	74.22	74.64
π C14- C15	1.620	1.616	1.615	π* C12- C13	0.295	0.274	0.274	99.83	93.14	93.14
π C14- C15	1.620	-	-	π* C7- N2	0.438	-	-	66.69	-	-
π C14- C15	-	1.616	1.615	π* C7- C8	-	0.316	0.317	-	56.48	56.40
π C11- N3	1.749	1.774	1.774	π* C14- C15	0.323	0.313	0.313	112.76	103.26	102.93
π C11- N3	1.749	1.774	1.774	π* C12- C13	0.295	0.274	0.274	48.07	43.05	43.14
π C12- C13	1.635	1.609	1.610	π* C14- C15	0.323	0.313	0.313	78.99	80.83	80.96
π C12- C13	1.635	1.609	1.610	π* C11- N3	0.378	0.404	0.404	138.36	153.76	153.34
π C6- C10	1.592	-	-	π* C7- N2	0.438	-	-	81.80	-	-
π C6- C10	1.592	-	-	π* C8- C9	0.300	-	-	102.42	-	-
π C6- C10	1.592	-	-	π* C3- C4	0.323	-	-	46.82	-	-
π C6- C10	-	1.758	1.757	π* C7- C8	-	0.316	0.317	-	106.69	106.57
π C6- C10	-	-	1.757	π* C9- C10	-	-	0.275	-	-	41.67
π C7- N2	1.722	-	-	π* C6- C10	0.329	-	-	117.95	-	-

π C7- N2	1.722	-	-	π* C8- C9	0.300	-	-	50.29	-	-
π C9- N10	-	1.599	1.599	π* C6- N2	-	0.488	0.487	-	157.44	156.27
π C9- N10	-	1.599	1.599	π* C7- C8	-	0.316	0.317	-	78.03	78.32
π C8- C9	1.634	-	-	π* C6- C10	0.329	-	-	76.86	-	-
π C8- C9	1.634	-	-	π* C7- N2	0.438	-	-	133.01	-	-
π C7- C8	-	1.586	1.585	π* C6- N2	-	0.488	0.487	-	79.96	80.92
π C7- C8	-	1.586	1.585	π* C9- C10	-	0.275	0.275	-	96.06	95.98
π C7- C8	-	1.586	1.585	π* C14- C15	-	0.313	0.313	-	49.79	49.83
π C3- C4	1.620	-	-	π* C6- C10	0.329	-	-	50.08	-	-
π C3- C4	-	1.616	1.615	π* C6- N2	-	0.488	0.487	-	84.22	83.55
π C3- C4	1.620	1.616	1.615	π* C2- N1	0.378	0.404	0.405	72.30	74.22	74.64
π C3- C4	1.620	1.616	1.615	π* C1- C5	0.295	0.274	0.274	99.83	93.14	93.14
π C2- N1	1.749	2.000	1.775	π* C3- C4	0.323	0.313	0.313	112.76	103.26	102.93
π C2- N1	1.749	2.000	1.775	π* C1- C5	0.295	0.274	0.274	48.07	43.05	42.93
π C1- C5	1.635	2.000	1.609	π* C3- C4	0.323	0.313	0.313	78.99	80.83	80.92
π C1- C5	1.635	2.000	1.609	π* C2- N1	0.378	0.404	0.405	138.36	153.76	153.85
σ O- H	-	-	1.998	4s Cu	-	-	0.344	-	-	0.79
sp^3 O	-	-	1.989	4s Cu	-	-	0.344	-	-	11.38
sp^3 O	-	-	1.509	4s Cu	-	-	0.344	-	-	0.54

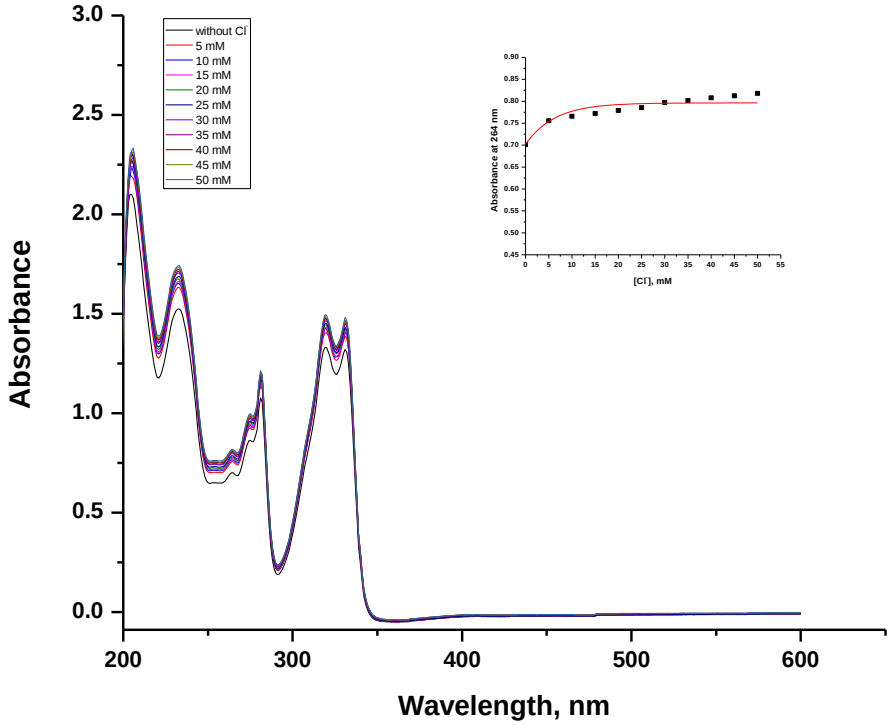

Figure S1. Effect of chloride concentration on spontaneous hydrolysis of the dichlorido [$ZnCl_2$(terpy)] complex. (UV/VIS is spectra of the complex (0.02 mmol L^{-1}) at pH 7.38 (0.005 mol L^{-1} phosphate buffer), recorded in the absence of NaCl (black line) and in the presence of the 5 mmol L^{-1} NaCl (red line), 10 mmol L^{-1} NaCl (blue line), 15 mmol L^{-1} NaCl (pink line) and etc. Intersept: dependence of the absorbance as a function of chloride concentration for the same reactions at 264 nm; red line presents the simulation of end of hydrolysis).

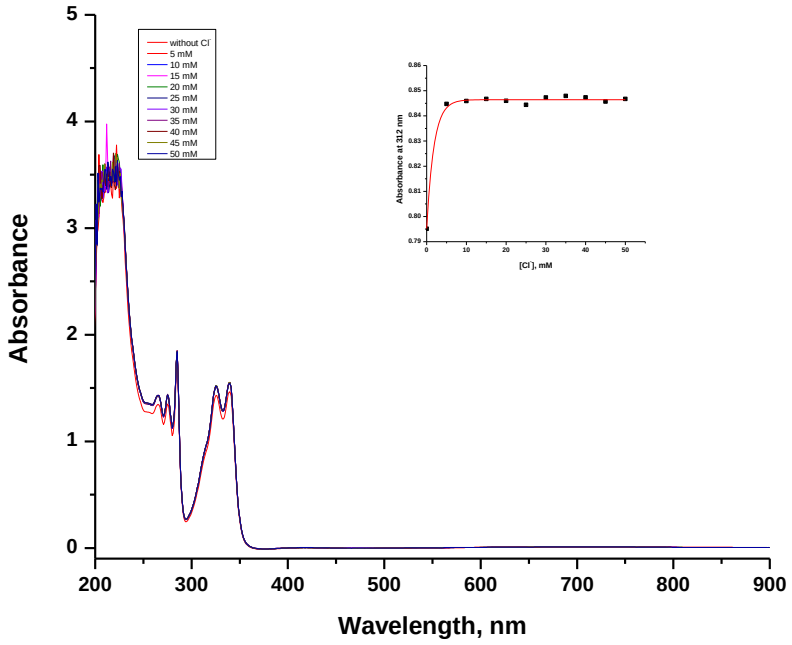

Figure S2. Influence of different chloride concentration on spontaneous hydrolysis of the dichlorido [$CuCl_2$(terpy)] complex. (UV/VIS is spectra of the complex (0.02 mmol L^{-1}) at pH 7.38 (0.005 mol L^{-1} phosphate buffer), recorded in the absence of NaCl (black line) and in the presence of the 5 mmol L^{-1} NaCl (red line), 10 mmol L^{-1} NaCl (blue line), 15 mmol L^{-1} NaCl (pink line) and etc. Intersept: dependence of the absorbance as a function of chloride concentration for the same reactions at 312 nm; red line presents the simulation of end of hydrolysis).

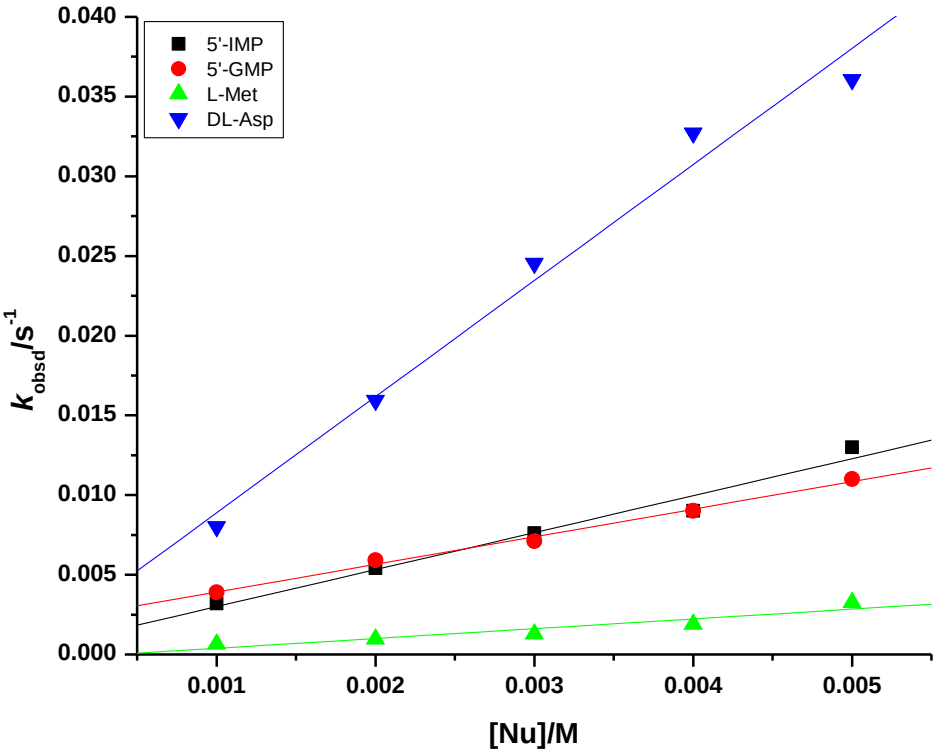

Figure S3. Pseudo-first order rate constants as a function of nucleophile concentration for the second reactions of the [$ZnCl_2$(terpy)] complex with L-Met, 5'-IMP, 5'-GMP and DL-Asp at at pH 7.38 (0.005 mol L^{-1} phosphate buffer) in the addition of 0.010 mol L^{-1} NaCl at 22°C.

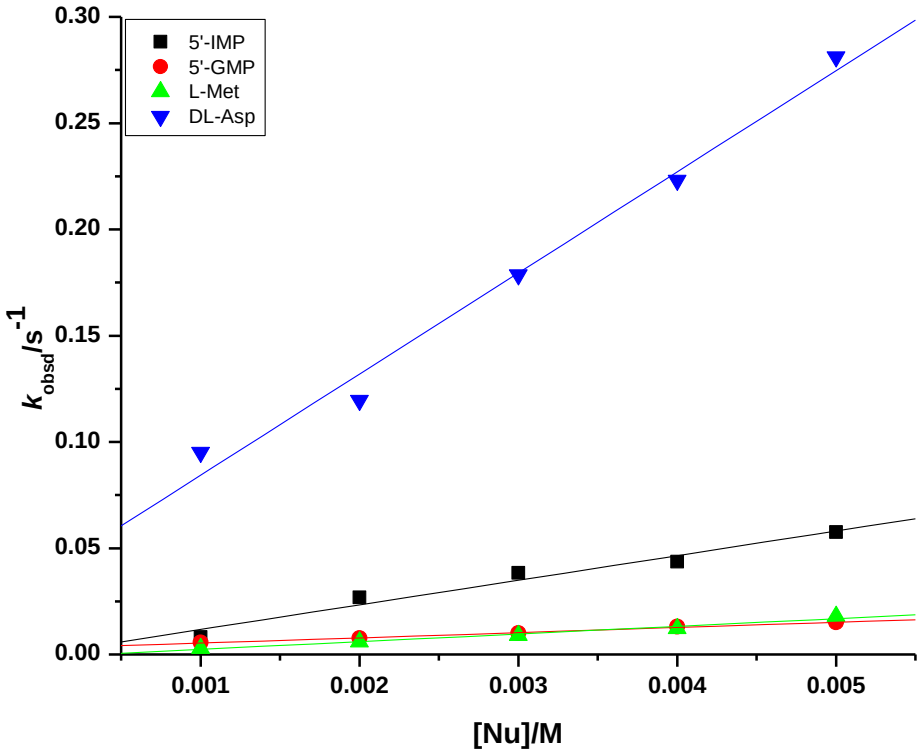

Figure S4. Pseudo-first order rate constants as a function of nucleophile concentration for the second reactions of the [$CuCl_2$(terpy)] complex with L-Met, 5'-IMP, 5'-GMP and DL-Asp at pH 7.38 (0.005 mol L^{-1} phosphate buffer) in the addition of 0.010 mol L^{-1} NaCl at 22°C.

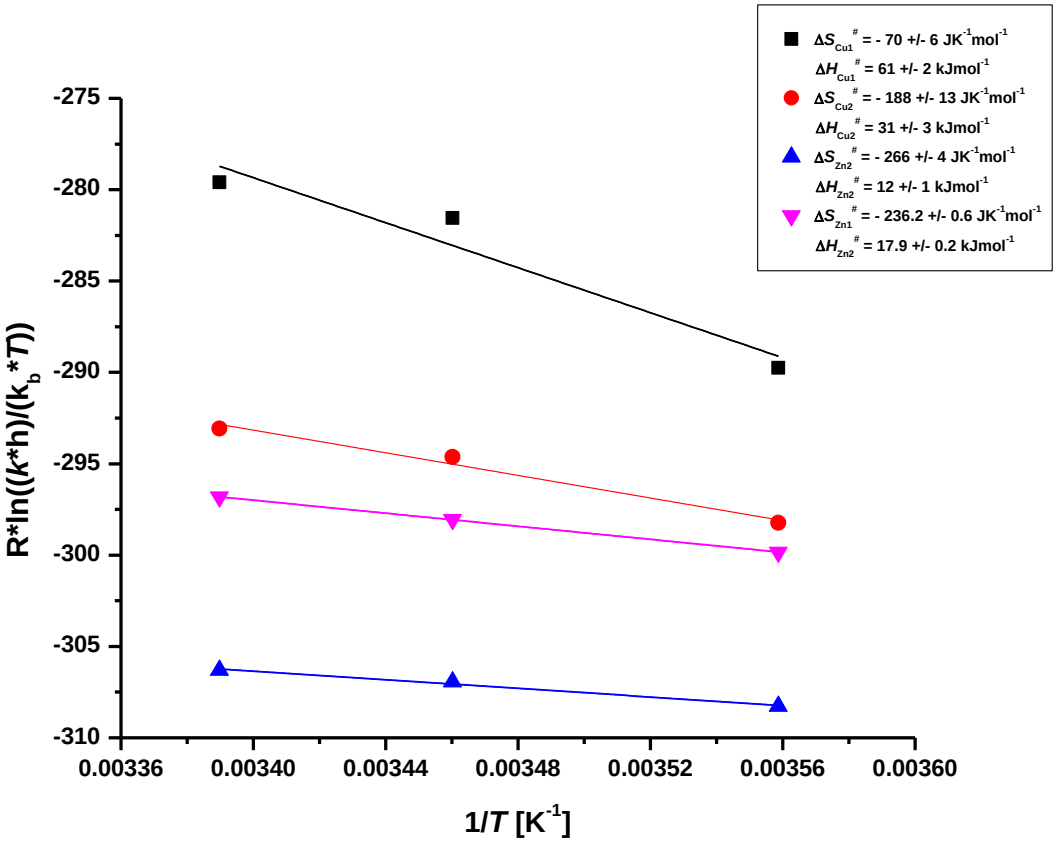

Figure S5. Eyring plots for the two reaction steps of [$CuCl_2$(terpy)] and [$ZnCl_2$(terpy)] complexes with L-methionine at pH 7.38 (0.005 mol L^{-1} phosphate buffer) in the addition of 0.010 mol L^{-1} NaCl.

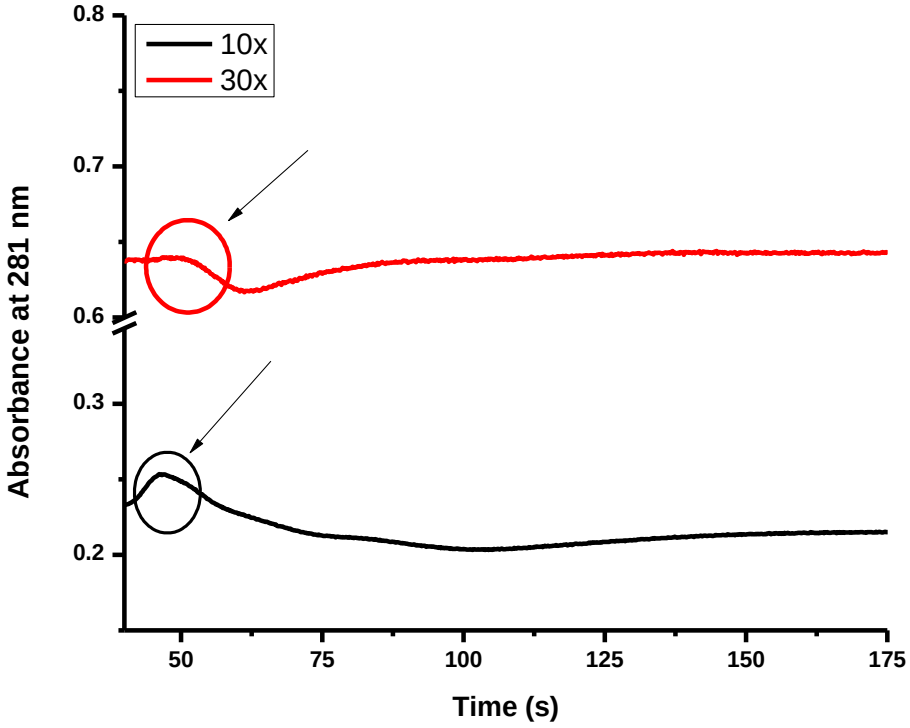

Figure S6. Time traces obtained for the reaction of 0.02 mmol L^{-1} GSH and 10 and 30-fold excess of the concentration of [$ZnCl_2$(terpy)] complexes at pH 7.38 (0.005 mol L^{-1} phosphate buffer) in the addition of 0.010 mol L^{-1} NaCl at 22°C at λ = 281 nm (The arrows points to the rise and fall in absorbance).

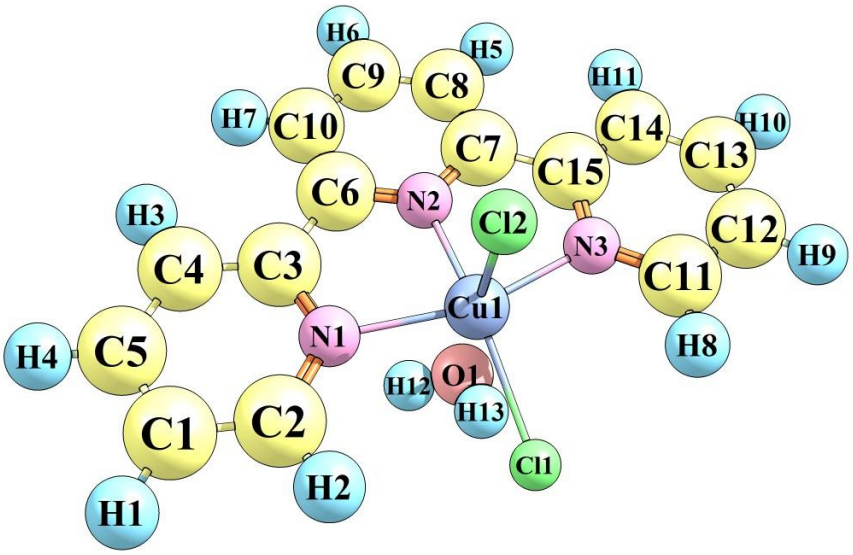

Figure S7. Atomic labeling of investigated $[CuCl_2(terpy)]\cdot H_2O$ complex. The same manner of the atoms labeling is valid for the complexes without the water molecule, as well as for Zn(II)$^-$ complexes.

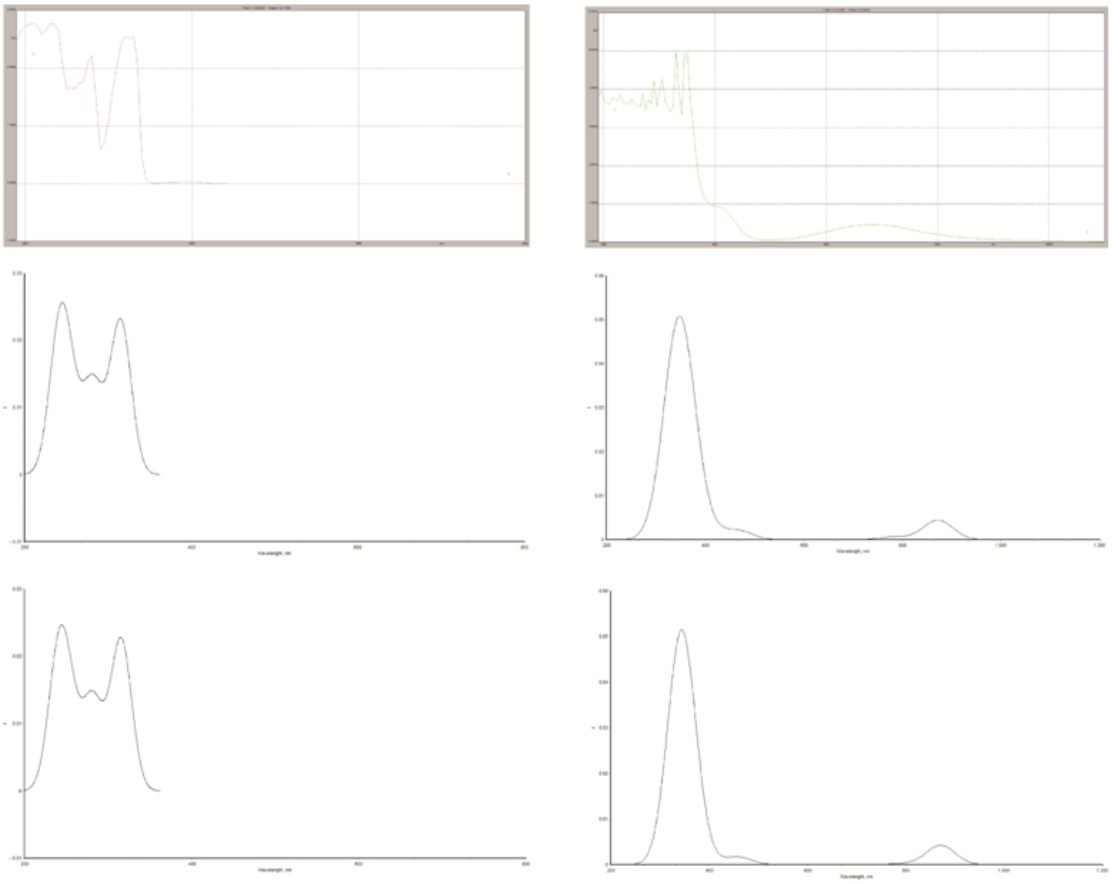

Figure S8. Experimental (up) and calculated (center and down) UV/Vis spectra of investigated Zn(II) complex (on the left) and Cu(II) (on the right). Spectra in the center are related to the corresponding non-hydrated complexes optimized in aqueous solution, while down spectra are related to the hydrated complexes.

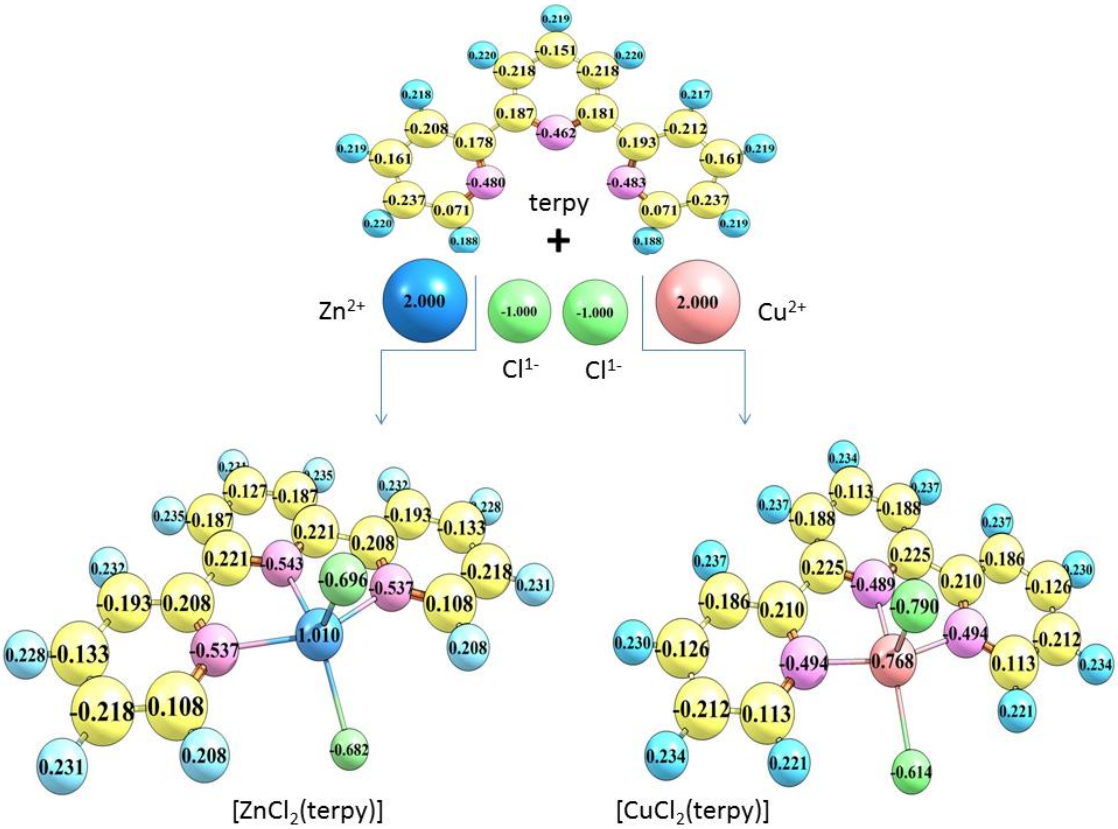

Figure S9. Changes of natural charge in ligands and central metal ions during complexation. Presented natural charges correspond to the moieties optimized in water as medium.